LETTER

doi:10.1038/nature12764

Origin and age of the earliest Martian crust from meteorite NWA 7533

M. Humayun[1], A. Nemchin[2]†, B. Zanda[3,4], R. H. Hewins[3,4], M. Grange[2], A. Kennedy[5], J.-P. Lorand[6], C. Göpel[7], C. Fieni[3], S. Pont[3] & D. Deldicque[8]

The ancient cratered terrain of the southern highlands of Mars is thought to hold clues to the planet's early differentiation[1,2], but until now no meteoritic regolith breccias have been recovered from Mars. Here we show that the meteorite Northwest Africa (NWA) 7533 (paired with meteorite NWA 7034[3]) is a polymict breccia consisting of a fine-grained interclast matrix containing clasts of igneous-textured rocks and fine-grained clast-laden impact melt rocks. High abundances of meteoritic siderophiles (for example nickel and iridium) found throughout the rock reach a level in the fine-grained portions equivalent to 5 per cent CI chondritic input, which is comparable to the highest levels found in lunar breccias. Furthermore, analyses of three leucocratic monzonite clasts show a correlation between nickel, iridium and magnesium consistent with differentiation from impact melts. Compositionally, all the fine-grained material is alkalic basalt, chemically identical (except for sulphur, chlorine and zinc) to soils from Gusev crater. Thus, we propose that NWA 7533 is a Martian regolith breccia. It contains zircons for which we measured an age of 4,428 ± 25 million years, which were later disturbed 1,712 ± 85 million years ago. This evidence for early crustal differentiation implies that the Martian crust, and its volatile inventory[4], formed in about the first 100 million years of Martian history, coeval with earliest crust formation on the Moon[5] and the Earth[6]. In addition, incompatible element abundances in clast-laden impact melt rocks and interclast matrix provide a geochemical estimate of the average thickness of the Martian crust (50 kilometres) comparable to that estimated geophysically[2,7].

NWA 7533 is a polymict breccia, characterized by a variety of clasts set in a fine-grained (~1 μm) interclast crystalline matrix (ICM) (Fig. 1). The main clast component consists of fine-grained (5–20 μm) clast-laden impact melt rock (CLIMR) occurring as oval or curved smooth bodies. Other clasts are made up of melt rock, melt spherules and fine-grained (20–100 μm) basaltic clasts, as well as lithic (noritic and monzonitic) and crystal (especially pyroxene and feldspar) clasts that occur in both melt rock and matrix (Fig. 1 and Supplementary Fig. 1). There is a surprising dearth of olivine in both matrix and clasts even though the Mg content of the matrix (~7.5%) is higher than that of Gusev crater soils. Among the lithic clasts are coarse-grained leucocratic rocks consisting of alkali feldspar, plagioclase, chlorapatite and ilmenite, with a monzonitic composition. Exsolution in both pyroxenes and alkali feldspars indicates that many lithic clasts are plutonic in origin (Supplementary Fig. 1). Chemical and oxygen isotopic[3] evidence confirms that NWA 7533 is a Martian meteorite (Supplementary Information). Here we present laser ablation ICP–MS (inductively coupled plasma mass spectrometry) elemental abundances and U–Pb zircon geochronology which demonstrate that NWA 7533 is a Martian regolith breccia, and discuss the implications of this result.

The ICM and CLIMR have abundances of Ni (400–700 p.p.m.) and Ir (10–80 p.p.b.) at their respective Mg contents (an index of chemical differentiation of basaltic liquids) that are much higher than those of shergottite–nakhlite–chassignite (SNC) meteorites (Ni < 200 p.p.m.; Ir < 1 p.p.b.) and comparable to those of lunar breccias[8,9] (Fig. 2), indicating a large meteoritic component. Moreover, the relative abundances of Ru, Rh and Os to Ir are in chondritic ratios in the ICM and CLIMR (Supplementary Fig. 2). The siderophile element contents of ICM and CLIMR require the equivalent of ~5% CI chondrite admixed into the Martian regolith. Prior explanations of the high Ni abundances in Gusev soils have included both indigenous[10] and meteoritic origins[11], but a chondritic impactor could not be inferred from Ni alone[11]. Surprisingly, the leucocratic clasts also have high Ni abundances relative to the SNC trend even at Mg < 0.1 wt%. The individual mineral spot analyses from two of the leucocratic clasts were examined after laser ablation ICP–MS analysis, and the spots were found to be contained entirely within the clast, not overlapping the Ni- and Ir-rich matrix (Supplementary Fig. 3). This is evidence that these leucocratic clasts

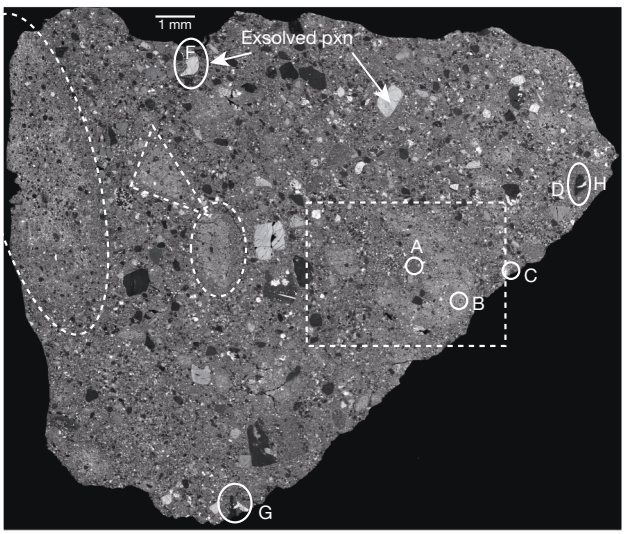

Figure 1 | Backscattered-electron image of NWA 7533 section 1. The breccia contains many large bodies of clast-laden impact melt rock (light or medium grey), some outlined with dot–dash lines, in fine-grained interclast crystalline matrix. Solid ellipses show crystal and lithic fragments, close-ups of which (lettered) are shown in Supplementary Information. Pyroxene (pxn; light or medium grey), feldspar (dark grey) and pyroxene–feldspar rock fragments are found in both melt rocks and matrix. Bright grey minerals include chlorapatite and Fe-rich oxides and oxyhydroxides.

[1]Department of Earth, Ocean and Atmospheric Science, and National High Magnetic Field Laboratory, Florida State University, Tallahassee, Florida 32310, USA. [2]Department of Applied Geology, Curtin University, Perth, Western Australia 6845, Australia. [3]Laboratoire de Minéralogie et Cosmochimie du Muséum, CNRS and Muséum National d'Histoire Naturelle, 75005 Paris, France. [4]Department of Earth and Planetary Sciences, Rutgers University, Piscataway, New Jersey 08854, USA. [5]Department of Applied Physics, Curtin University, Perth, Western Australia 6845, Australia. [6]Laboratoire de Planétologie et Géodynamique de Nantes, CNRS UMR 6112, Université de Nantes, 2 Rue de la Houssinière, BP 92208, 44322 Nantes Cedex 3, France. [7]Institut de Physique du Globe, Sorbonne Paris Cité, University Paris Diderot, CNRS UMR 7154, F-75005 Paris, France. [8]Ecole Normale Supérieure, UMR 8538, 75231 Paris Cedex 5, France. †Present address: Laboratory for Isotope Geology, Swedish Museum of Natural History, SE-104 05 Stockholm, Sweden.

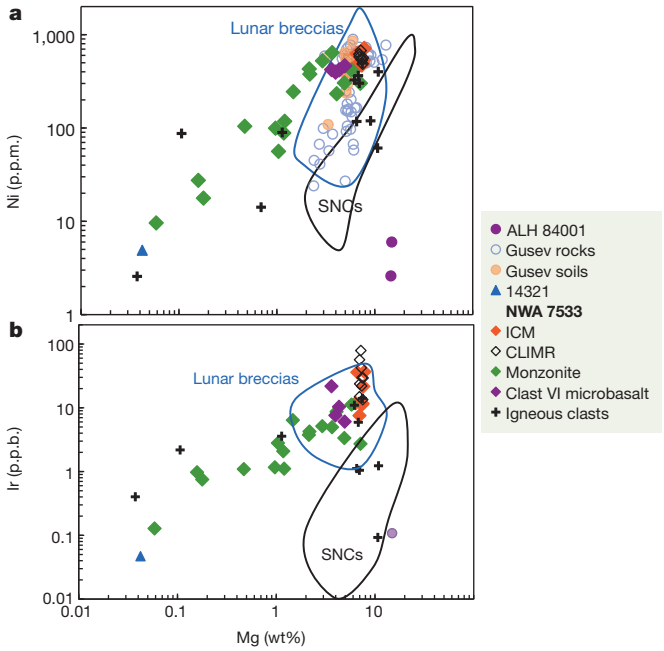

Figure 2 | Siderophile-element abundances in NWA 7533. a, Ni versus Mg, comparing abundances in NWA 7533 components with those in Gusev rocks and soils[12,13], other Martian meteorites (SNCs[23] and ALH 84001[24,25]), Apollo 15–17 breccias[26–28] and lunar meteorites[8,9], and a lunar felsite, 14321, c4 (ref. 29). **b**, Ir versus Mg for the same samples (excluding Gusev rocks and soils, for which Ir data are not available). For literature sources, see above. Some of the *in situ* analyses from NWA 7533 are higher in Ir than any of the lunar breccias, owing to the influence of Ir-rich nuggets.

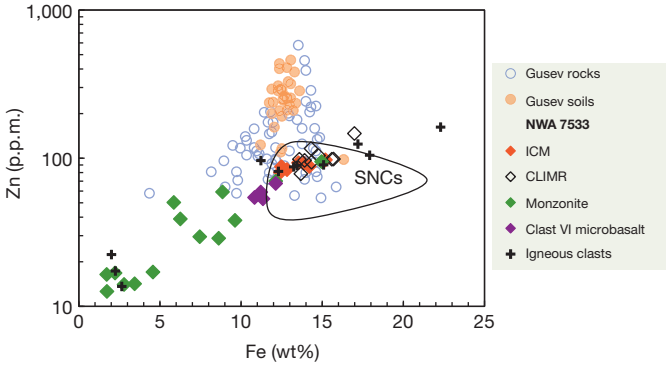

Figure 3 | Gusev rock and soil analyses[13] have systematically higher Zn abundances than both Martian meteorites and NWA 7533. Pyroxene-rich nakhlites and ALH 84001 are higher in Zn than are olivine-rich chassignites, but none of the known nakhlites is as Fe-rich as some of the igneous-textured clasts from NWA 7533, which extend beyond the SNC field to higher Fe. Together with S and Cl, Zn abundances are systematically enriched in modern soils relative to NWA 7533, presumably because of the lack of liquid water on modern Mars.

crystallized from impact melts enriched in siderophile elements to concentrations similar to those in the ICM and CLIMR.

The remarkable chemical similarity between NWA 7034[3] and Gusev rock and soil analyses[12,13] is confirmed here for NWA 7533. Abundances of major elements (Si, Al, Fe, Ca and Na) in CLIMR and ICM are identical to those in Gusev soils, except for higher Mg in CLIMR and ICM (Supplementary Fig. 4). Among minor elements, the similarity of CLIMR and ICM to Gusev soils is evident in Ni (Fig. 2), Ti and K, although P is up to twice as high as in Gusev soils owing to the abundant chlorapatite in NWA 7533. The fine-grained textures and uniform chemical composition of CLIMR and ICM, which resembles the ubiquitous soil composition reported by NASA's Viking[14], Pathfinder[15] and Mars Exploration Rover[12,13] missions, indicate that these materials contain important amounts of wind-blown dust. Because Ni is a reliable tracer for soil, Gusev rocks with high Ni contents[12,13] may be lithified sediments or impact breccias and cannot be regarded as basalts[10]. Unlike modern Martian soils[11–15], ICM and CLIMR do not show enrichments of S, Cl and Zn with values similar to SNC meteorites (Fig. 3). These elements are likely to be in water-soluble phases in modern soils and the lack of enrichment observed in NWA 7533 components is probably due to the transportation of these salts into ancient seas or lakes[16] by liquid water present on Mars at the time of formation of ICM and CLIMR.

Rare-earth element (REE) abundances for ICM are identical in pattern to those for CLIMR, indicating that the two fine-grained lithologies in this meteorite are derived from similar precursors (Fig. 4). The REE pattern for ICM and CLIMR in NWA 7533 agrees well with the pattern previously reported for bulk NWA 7034[3], except that our *in situ* analyses are less contaminated with leucocratic clasts that carry a striking negative Eu anomaly (Fig. 4). The absolute enrichment of REE varies from 40 to 46 times the CI chondrite level owing to the ubiquitous presence of 10–100-μm clasts in all the analyses. Some of these clasts contribute small Eu anomalies, in the absence of which the REE patterns of the CLIMR and ICM from NWA 7533 would be smooth and depleted in heavy REEs.

The chemical composition of Martian wind-blown dust, present as ICM and CLIMR in NWA 7533, should provide clues to the original igneous processes that formed the primary Martian crust. A partial-melting model of a primitive mantle composition for Mars (Supplementary Information) indicates that a ~4% partial melt of a fertile mantle containing <1% garnet provides a fit to the CLIMR and ICM REE patterns (Fig. 4). The exact value of the melt fraction depends on the absolute REE abundances, which are diluted by the presence of clasts. If this melt were extracted from the entire Martian mantle it would form a uniform global layer 50 km thick, which is incidentally identical to the average thickness of the Martian crust inferred from gravity and topography measurements by NASA's Mars Global Surveyor[7]. The absence of a garnet (majorite) signature argues against formation of this enriched material as the last dregs of a magma ocean. Combined ^{142}Nd–^{143}Nd isotope evidence in shergottites implies that the formation of the enriched and depleted reservoirs on Mars occurred within the first

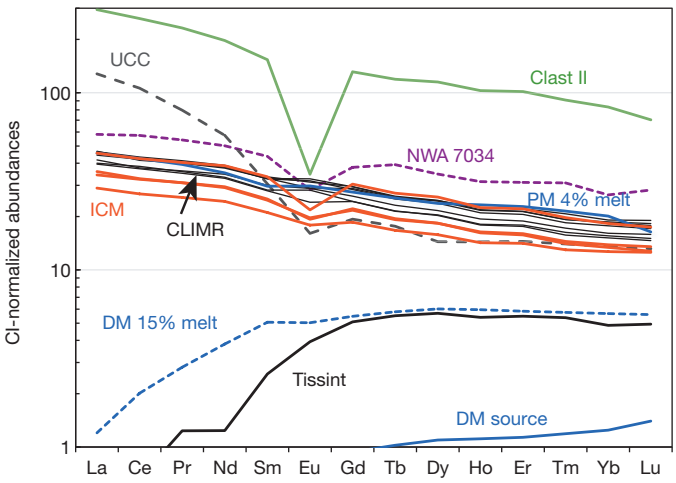

Figure 4 | REE patterns for the representative components of NWA 7533 including the fine-grained ICM and CLIMR. The previously reported bulk REE analysis of NWA 7034[3] (purple) represents a mixture between the ICM or CLIMR and clasts such as monzonite clast II (green). Earth's upper continental crust[30] (UCC) is shown for comparison. The blue curves depict model results: a 4% partial melt of primitive Martian mantle (PM) and the complementary residue termed the depleted Martian source (DM); a higher degree melt (15%) of the DM source; and Tissint[19], a depleted shergottite.

100 Myr of the planet's history[17]. Here we identify the enriched reservoir to be the crust. It is no longer necessary to invoke a magma ocean from Nd isotope evidence for Mars[18], and we take the 100-Myr Nd isotope timescale to imply that the Martian crust formed very early. Removal of this primary melt yields a depleted residue (Fig. 4), which, on subsequent melting (~15%), yields a composition like that of Tissint meteorite[19], a depleted shergottite. Crustal assimilation by depleted-shergottite magmas then gives rise to intermediate and enriched shergottites[3].

NWA 7533 contains numerous evolved igneous clasts that contain zircons. These evolved lithologies (monzonitic or mugearitic[20] magmas) probably formed by re-melting of the primary Martian crust either at depth in the presence of volatiles[20] or by differentiation of large impact melt sheets. Sensitive high-resolution ion microprobe (SHRIMP) dating of these zircons (Fig. 5) provides a powerful lower limit on the timescale of crustal differentiation. The zircon grains were from 6–70 μm and the spot size for the SHRIMP was ~7 μm in diameter; as a result, some of the analysed spots overlapped the matrix (Supplementary Information and Supplementary Fig. 5). The analyses of overlapping spots were excluded. The analyses for five of ten investigated grains that were entirely within zircon fall on a single discordia line with an upper intercept of 4,428 ± 25 Myr (1σ) and a lower intercept of 1,712 ± 85 Myr (1σ) (Fig. 5). The mean squared weighted deviation, of 2.4, most probably results from the analyses being performed on a polished section with some variability in relief, yielding excess scatter of calculated U/Pb in the sample compared with the standard. All analyses, with the exception of two, show $^{206}Pb/^{204}Pb > 400$, with a maximum value of ~1,600 (Supplementary Information). Although these ratios are lower than those usually observed in terrestrial zircons of the same age[6], the common-Pb correction was insensitive to the choice of common-Pb composition. A single, nearly concordant zircon (Z11) with a $^{207}Pb/^{206}Pb$ age of 4114 ± 30 Myr (1σ) may represent a different age population of zircons in the sample.

These ancient ages for Martian zircons are strikingly similar to the ages of the earliest terrestrial[6] and lunar zircons[5], implying coeval crust formation on the Earth, Moon and Mars. Because the leucocratic clasts formed either by impact or by internal melting of the crust, the events dated by the zircons post-date the emplacement of the Martian crust (4.47 Gyr (ref. 17)) by only ~40 Myr. The cause of the younger age intercept at 1.7 Gyr is not known, but it is close to the Rb–Sr age of 2.1 Gyr for NWA 7034[3], indicating major disturbance of both U–Pb and Rb–Sr ages for the leucocratic clasts at this time.

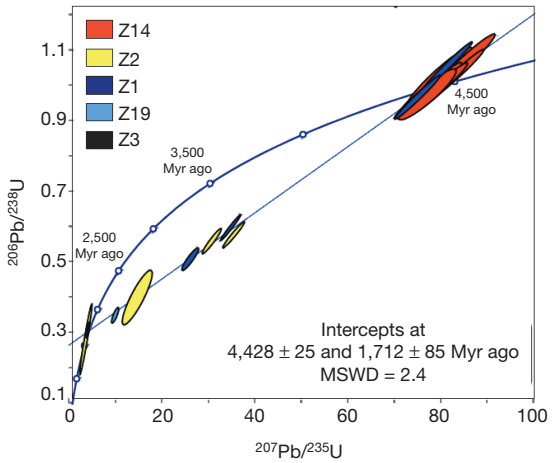

Figure 5 | Concordia plot for SHRIMP analysis of five zircon grains from NWA 7533 section 4 defines a discordia line. Data error ellipses are 2σ. Analyses from three zircons plot on the upper intercept (Z1, Z14, Z15), and the analysis from one grain plots on the lower intercept (Z3). MSWD, mean squared weighted deviation.

The combination of compositional and chronological evidence presented here for NWA 7533 implies that it originated from the earliest Martian crust brecciated by impacts. The alkali basalt composition of this crust is now ubiquitously distributed by impacts and wind-blown dust in all major Martian soils sampled by spacecraft landers[11–15]. The observation that Ni remains as high in modern soils as in CLIMR implies minimal subsequent crustal resurfacing on Mars. Evidence for early differentiation (>4,400 Myr ago) within the crust to form leucocratic rocks, and the redistribution of these clasts into highland breccias, forms a potent means by which large areas of Martian crust can retain K/Th signatures distinct from that of the uniform wind-blown dust[21]. The early magmatic build-up of the Martian highland crust requires an equally rapid release of volatiles from the Martian interior, forming the early atmosphere and hydrosphere of Mars[1,4], with implications for early Martian climate and biological potential[22]. Further studies of this meteorite will shed light on plutonic rock compositions of the Martian highlands, Martian zirconology and the earliest sedimentary compositions on Mars.

METHODS SUMMARY

Samples of NWA 7533 were analysed using a Tescan VEGA II LSU scanning electron microscope and a Zeiss SIGMA scanning electron microscope at MNHN Paris and ENS Paris, and a CAMECA SX5 electron microprobe at the Université Paris VI. An uncoated section, NWA 7533 section 3, was analysed by laser ablation ICP–MS using an ElectroScientific Instruments New Wave UP193FX ArF excimer (193 nm) laser ablation system coupled to a Thermo Electron Element XR ICP–MS at Florida State University. Altogether, 76 peaks for major and trace elements and their interferences were monitored. Spot sizes of 50–150 μm were used, and the laser repetition rate was 50 Hz, with a fluence of >2 GW cm^{-2}. Raster rates were 10 μm s^{-1}. Laser dwell times on a spot were 20 s, resulting in a pit depth of ~100 μm. Relative sensitivity factors obtained from separate standards for many well-characterized lithophile elements agreed to 2–5%, but the accuracy was worse for elements for which only one standard was available, for example NIST SRM 610 (~10–20%). Before U–Pb analysis, zircons were imaged by cathodoluminescence using a variable-pressure Zeiss EVO scanning electron microscope at Curtin University configured to collect a cathodoluminescence signal, with an acceleration voltage of 10 kV. The working distance was 8.5 mm. Uranium–lead isotope analyses on Au-coated NWA 7533 section 4 were performed on a SHRIMP II at Curtin University under analytical conditions described previously[5]. The beam spot was reduced to 7 μm to effectively analyse the small zircons observed with a primary O^{2-} beam current of 0.5 nA (Methods).

Online Content Any additional Methods, Extended Data display items and Source Data are available in the online version of the paper; references unique to these sections appear only in the online paper.

Received 4 July; accepted 10 October 2013.
Published online 20 November 2013.

1. Solomon, S. C. *et al.* New perspectives on ancient Mars. *Science* **307,** 1214–1220 (2005).
2. Nimmo, F. & Tanaka, K. Early crustal evolution of Mars. *Annu. Rev. Earth Planet. Sci.* **33,** 133–161 (2005).
3. Agee, C. B. *et al.* Unique meteorite from early Amazonian Mars: water-rich basaltic breccia Northwest Africa 7034. *Science* **339,** 780–785 (2013).
4. Marty, B. & Marti, K. Signatures of early differentiation of Mars. *Earth Planet. Sci. Lett.* **196,** 251–263 (2002).
5. Nemchin, A. *et al.* Timing of crystallization of the lunar magma ocean constrained by the oldest zircon. *Nature Geosci.* **2,** 133–136 (2009).
6. Wilde, S. A., Valley, J. W., Peck, W. H. & Graham, C. M. Evidence from detrital zircons of the existence of continental crust and oceans on the Earth 4.4 Gyr ago. *Nature* **409,** 175–178 (2001).
7. Zuber, M. T. *et al.* Internal structure and early thermal evolution of Mars from Mars Global Surveyor topography and gravity. *Science* **287,** 1788–1793 (2000).
8. Korotev, R. L., Ziegler, R. A., Jolliff, B. L., Irving, A. J. & Bunch, T. E. Compositional and lithological diversity among brecciated lunar meteorites of intermediate iron concentrations. *Meteorit. Planet. Sci.* **44,** 1287–1322 (2009).
9. Warren, P. H., Ulff-Møller, F. & Kallemeyn, G. W. "New" lunar meteorites: impact melt and regolith breccias and large-scale heterogeneities of the upper lunar crust. *Meteorit. Planet. Sci.* **40,** 989–1014 (2005).
10. Tuff, J., Wade, J. & Wood, B. J. Volcanism on Mars controlled by early oxidation of the upper mantle. *Nature* **498,** 342–345 (2013).
11. Yen, A. S. *et al.* An integrated view of the chemistry and mineralogy of Martian soils. *Nature* **436,** 49–54 (2005).
12. McSween, H. Y., Taylor, G. J. & Wyatt, M. B. Elemental composition of the Martian crust. *Science* **324,** 736–739 (2009).

13. Gellert, R. *et al.* Alpha Particle X-Ray Spectrometer (APXS): results from Gusev crater and calibration report. *J. Geophys. Res.* **111,** E02S05 (2006).
14. Clark, B. C. *et al.* Chemical composition of Martian fines. *J. Geophys. Res.* **87,** 10,059–10,067 (1982).
15. Foley, C. N., Economou, T. & Clayton, R. N. Final chemical results from the Mars pathfinder alpha proton X-ray spectrometer. *J. Geophys. Res.* **108,** 8096 (2003).
16. Di Achille, G. & Hynek, B. A. Ancient ocean on Mars supported by global distribution of deltas and valleys. *Nature Geosci.* **3,** 459–463 (2010).
17. Debaille, V., Brandon, A. D., Yin, Q.-Z. & Jacobsen, B. Coupled ^{142}Nd-^{143}Nd evidence for a protracted magma ocean in Mars. *Nature* **450,** 525–528 (2007).
18. Elkins-Tanton, L. T. Magma oceans in the inner solar system. *Annu. Rev. Earth Planet. Sci.* **40,** 113–139 (2012).
19. Aoudjehane, H. C. *et al.* Tissint Martian meteorite: a fresh look at the interior, surface, and atmosphere of Mars. *Science* **338,** 785–788 (2012).
20. Stolper, E. M. *et al.* The petrochemistry of Jake_M: a Martian mugearite. *Science* **341,** 1239463 (2013).
21. Taylor, G. J. *et al.* Variations in K/Th on Mars. *J. Geophys. Res.* **111,** E03S06 (2006).
22. Jakosky, B. M. & Phillips, R. J. Mars' volatile and climate history. *Nature* **412,** 237–244 (2001).
23. Brandon, A. D. *et al.* Evolution of the Martian mantle inferred from the ^{187}Re-^{187}Os isotope and highly siderophile element abundance systematics of shergottite meteorites. *Geochim. Cosmochim. Acta* **76,** 206–235 (2012).
24. Warren, P. H., Kallemeyn, G. W. & Kyte, F. T. Origin of planetary cores: Evidence from highly siderophile elements in martian meteorites. *Geochim. Cosmochim. Acta* **63,** 2105–2122 (1999).
25. Kong, P., Ebihara, M. & Palme, H. Siderophile elements in Martian meteorites and implications for core formation in Mars. *Geochim. Cosmochim. Acta* **63,** 1865–1875 (1999).
26. Norman, M. D., Bennett, V. C. & Ryder, G. Targeting the impactors: siderophile element signatures of lunar impact melts from Serenitatis. *Earth Planet. Sci. Lett.* **202,** 217–228 (2002).
27. Palme, H. *et al.* New data on lunar samples and achondrites and a comparison of the least fractionated samples from the Earth, the Moon and the Eucrite parent body. *Proc. Lunar Sci. Conf.* **9,** 25–57 (1978).
28. Wänke, H. *et al.* On the chemistry of lunar samples and achondrites: Primary matter in the lunar highlands. A re-evaluation. *Proc. Lunar Sci. Conf.* **8,** 2191–2213 (1977).
29. Warren, P. H., Taylor, G. J., Keil, K., Shirley, D. N. & Wasson, J. T. Petrology and chemistry of two ''large'' granite clasts from the Moon. *Earth Planet. Sci. Lett.* **64,** 175–185 (1983).
30. Rudnick, R. L. & Gao, S. in *Treatise on Geochemistry* Vol. 3, *The Continental Crust* (ed. Rudnick, R. L.) 1–64 (Elsevier-Pergamon, 2003).

Supplementary Information is available in the online version of the paper.

Acknowledgements We thank L. Labenne for providing samples of NWA 7533 for this study. We thank M. Fialin and F. Couffignal for help with the electron microprobe. We thank the NASA Cosmochemistry Program for support to M.H. (NNX10AI37G) and the Programme National de Planétologie, France, for support to B.Z. M.G. thanks the ARC Centre of Excellence CCFS for funding. We thank H. McSween for comments.

Author Contributions M.H., A.N., B.Z. and R.H.H. had the idea behind and directed the research, and wrote the manuscript. M.H. and B.Z. performed laser ablation ICP–MS analyses at Florida State University; A.N., M.G. and A.K. performed the SHRIMP ion probe U–Pb analyses at Curtin University and interpreted the chronology; B.Z. and C.F. prepared polished samples; R.H.H. and B.Z. performed petrological studies; J.-P.L. and S.P. investigated the mineralogy of the sulphide phases and searched for the carriers of platinum-group elements; C.G. provided separated CLIMR clasts; S.P., D.D., J.-P.L. and B.Z. located and imaged zircon and baddeleyite by scanning electron microscopy.

Author Information Reprints and permissions information is available at www.nature.com/reprints. The authors declare no competing financial interests. Readers are welcome to comment on the online version of the paper. Correspondence and requests for materials should be addressed to M.H. (humayun@magnet.fsu.edu).

METHODS

Laser ablation ICP–MS measurements of NWA 7533. An uncoated section, NWA 7533 section 3, was analysed by laser ablation ICP–MS using an Electro-Scientific Instruments New Wave UP193FX ArF excimer (193 nm) laser ablation system coupled to a Thermo Electron Element XR ICP–MS at Florida State University, as described elsewhere[31–33]. Spot sizes of 50–150 μm were used, the laser repetition rate was 50 Hz and the fluence was $>2\,GW\,cm^{-2}$. Raster rates were $10\,\mu m\,s^{-1}$. Laser dwell times on a spot were 20 s, resulting in a pit depth of ~100 μm. Altogether, 76 peaks for major and trace elements and their interferences were monitored, and the intensities converted to concentrations using a combination of silicate, sulphide and metal standards, including NIST SRM 610 glass[34]; USGS glasses BHVO-2g, BCR-2g and BIR-1g; NIST SRM 1263a steel[35]; Hoba[36] (IVB); North Chile (Filomena, IIA); and a pyrite crystal. The MPI-DING glasses were measured as independent controls. Major elements were determined using published methods[37]. Relative sensitivity factors obtained from separate standards for many well-characterized lithophile elements agreed to 2–5%, but the accuracy is worse for elements for which only one standard was available, for example NIST SRM 610 (~10–20%). Interference corrections for doubly charged Ba, Nd and Sm ions on Zn, Ga, Ge, As and Se were performed by monitoring $^{137}Ba^{2+}$, $^{145}Nd^{2+}$ and $^{149}Sm^{2+}$. Owing to interference from ZrO^+ and MoO^+, no data are reported for Pd, Ag and Cd here. The absence of suitable standards prevented data from being obtained for Br, I and Hg. Representative chemical compositions for selected samples discussed in the text, peaks monitored and detection limits determined on MPI-DING glasses are provided in Supplementary Table 1, together with the bulk composition of NWA 7034[3]. Section 3 was then carbon-coated and examined by EMP in Paris. Examples of post-ablation images are provided in Supplementary Fig. 3.

SHRIMP U–Pb analyses of zircon and baddeleyite. Before U–Pb analysis, zircons were imaged by cathodoluminescence using a variable-pressure Zeiss EVO scanning electron microscope at Curtin University configured to collect a cathodoluminescence signal, with an acceleration voltage of 10 kV. The working distance was 8.5 mm. Uranium–lead isotope analyses on Au-coated NWA 7533 section 4 were performed on a SHRIMP II at Curtin University under analytical conditions described previously[38–40]. The beam spot was reduced to 7 μm using a 30-μm Kohler aperture to effectively analyse the small zircons observed with a primary O^{2-} beam current of 0.5 nA. Secondary ions were passed to the mass spectrometer operating at a mass resolution ($M/\Delta M$ at 1%) of ~5,000. Each analysis was preceded by a 2-min raster to remove the Au coating and surface contamination. The peak-hopping U–Pb data collection routine consisted of seven scans through the mass stations, with signals measured using an ion-counting electron multiplier. Compared with a typical zircon ion probe analysis, counting times were increased for ^{204}Pb (to 20 s), ^{206}Pb (to 20 s) and ^{207}Pb (to 50 s) to increase the precision of $^{207}Pb/^{206}Pb$ for individual spot analyses. The sensitivity of the instrument during the session was determined to be 20 c.p.s. p.p.m.$^{-1}$ nA^{-1} using Pb isotopes. Measured Pb/U and Pb/Th ratios in zircon grains were corrected using a 562-Myr-old CZ3 zircon standard[41]. Twenty seven analyses of this standard made during the session resulted in an external error of 2.4% (1σ) in $^{206}Pb/^{238}U$, which was added to the errors in $^{206}Pb/^{238}U$ obtained for each Martian zircon.

Considering that SHRIMP analyses of U/Pb in baddeleyite suffer from strong orientation effects, preventing reliable estimates of U/Pb (ref. 42), only $^{207}Pb/^{206}Pb$ ages have been calculated for three baddeleyite grains identified in the section (Supplementary Fig. 6). Common Pb in both zircon and baddeleyite was corrected using present-day terrestrial ratios[43], following the observation that much of the common Pb in sections of extraterrestrial materials comes from contamination of the samples during their preparation[44]. However, correcting all analyses using more primitive Pb isotope compositions does not result in any meaningful change in the calculated ages. Raw data have been reduced using SQUID2[45]. Concordia diagrams and intercept calculations were made using Excel add-in ISOPLOT3.75[46]. The calculated data are presented in the Supplementary Table 2 with errors reported at the 1σ level. Ellipses and error bars in all diagrams are shown at the 2σ level and intercept ages are calculated at the 95% confidence level.

31. Humayun, M., Simon, S. B. & Grossman, L. Tungsten and hafnium distribution in calcium-aluminum inclusions (CAIs) from Allende and Efremovka. *Geochim. Cosmochim. Acta* **71,** 4609–4627 (2007).
32. Gaboardi, M. & Humayun, M. Elemental fractionation during LA-ICP-MS analysis of silicate glasses: implications for matrix-independent standardization. *J. Anal. Atomic Spectrom.* **24,** 1188–1197 (2009).
33. Humayun, M. Chondrule cooling rates inferred from diffusive profiles in metal lumps from the Acfer 097 CR2 chondrite. *Meteor. Planet. Sci.* **47,** 1191–1208 (2012).
34. Jochum, K. P. *et al.* Determination of reference values for NIST SRM 610-617 glasses following ISO guidelines. *Geostand. Geoanalyt. Res.* **35,** 397–429 (2011).
35. Campbell, A. J., Humayun, M. & Weisberg, M. K. Siderophile element constraints on the formation of metal in the metal-rich chondrites Bencubbin, Weatherford, and Gujba. *Geochim. Cosmochim. Acta* **66,** 647–660 (2002).
36. Walker, R. J. *et al.* Modeling fractional crystallization of group IVB iron meteorites. *Geochim. Cosmochim. Acta* **72,** 2198–2216 (2008).
37. Humayun, M., Davis, F. A. & Hirschmann, M. M. Major element analysis of natural silicates by laser ablation ICP-MS. *J. Anal. Atomic Spectrom.* **25,** 998–1005 (2010).
38. Compston, W., Williams, I. S. & Meyer, C. U–Pb geochronology of zircons from Lunar Breccia 73217 using a sensitive high mass-resolution ion microprobe. *J. Geophys. Res.* **89,** 525–534 (1984).
39. Nelson, D. R. Compilation of SHRIMP U-Pb geochronology data, 1996. *Geol. Surv. West. Aust. Rec.* **1997/ 2,** 1–11 (1997).
40. Williams, I. S. in *Applications of Microanalytical Techniques to Understanding Mineralising Processes* (eds McKibben, M. A., Shanks, W. C. & Riley, W. I.) 1–35 (Rev. Econ. Geol. 7, Society of Economic Geologists, 1998).
41. Pidgeon, R. T., Furfaro, D., Kennedy, A. K., Nemchin, A. A. & van Bronswjk, W. Calibration of zircon standards for the Curtin SHRIMP. *US Geol. Surv. Circ.* **1107,** 251 (1994).
42. Wingate, M. T. D. & Compston, W. Crystal orientation effects during ion microprobe U-Pb analysis of baddeleyite. *Chem. Geol.* **168,** 75–97 (2000).
43. Stacey, J. S. & Kramers, J. D. Approximation of terrestrial lead isotope evolution by a two-stage model. *Earth Planet. Sci. Lett.* **26,** 207–221 (1975).
44. Nemchin, A. A., Pidgeon, R. T., Whitehouse, M. J., Vaughan, J. P. & Meyer, C. SIMS U-Pb study of zircon from Apollo 14 and 17 breccias: implications for the evolution of lunar KREEP. *Geochim. Cosmochim. Acta* **72,** 668–689 (2008).
45. Ludwig, K. R. *User's Manual for Isoplot 3.60: A Geochronological Toolkit for Microsoft Excel.* Spec. Publ. 4 (Berkeley Geochronological Center, 2008).
46. Ludwig, K. R. *Squid 2 – A User's Manual (rev 2.50).* Spec. Publ. 4 (Berkeley Geochronology Center, 2009).